

See discussions, stats, and author profiles for this publication at: <https://www.researchgate.net/publication/230328037>

Effect of hydrogen bonding on the physical and mechanical properties of rigid-rod polymers

ARTICLE *in* JOURNAL OF POLYMER SCIENCE PART B POLYMER PHYSICS · DECEMBER 2000

Impact Factor: 3.83 · DOI: 10.1002/1099-0488(20001201)38:23<3053::AID-POLB70>3.0.CO;2-H

CITATIONS

16

READS

35

3 AUTHORS, INCLUDING:



Shawn Jenkins

Kimberly-Clark Corporation

14 PUBLICATIONS 141 CITATIONS

SEE PROFILE

The Effect of Hydrogen Bonding on the Physical and Mechanical Properties of Rigid-Rod Polymers

SHAWN JENKINS, KARL I. JACOB, SATISH KUMAR

School of Textile and Fiber Engineering, Georgia Institute of Technology, Atlanta, Georgia 30332-0295

Received 28 April 2000; revised 24 August 2000; accepted 30 August 2000

ABSTRACT: The idea of competing effects between intramolecular and intermolecular hydrogen bonding was investigated. Results indicate that the formation of one type of hydrogen bond does not preclude the formation of the other. The strength of the intermolecular association was measured by *ab initio* calculations for several polymer systems, including methyl pendant poly(*p*-phenylene benzobisimidazole) and poly-{2,6-diimidazo[4,5-*b*:4'5'-*e*]pyridinylene-1,4(2,5-dihydroxy)phenylene} (PIPD). Fibers with strong intermolecular association have high compressive strength and torsional modulus. The influence of intermolecular hydrogen bonding on torsional modulus is discussed in light of the transverse texture present in poly(*p*-phenylene terephthalamide) and some other high-performance fibers. Enhanced intermolecular interaction not only influences the aforementioned properties but also results in higher fiber density. © 2000 John Wiley & Sons, Inc. *J Polym Sci B: Polym Phys* 38: 3053–3061, 2000

Keywords: hydrogen bonding; rigid-rod polymers; compressive strength; torsional modulus; methyl pendant poly(*p*-phenylene benzobisimidazole) (MePBI); PIPD

INTRODUCTION

The introduction of hydrogen bonds in high-performance polymers has been attempted as a means to improve compressive strength.¹ The somewhat higher compressive strength of poly(*p*-phenylene terephthalamide) (PPTA)² compared with the strength of fibers such as poly(*p*-phenylene benzobisoxazole) (PBO) and poly(*p*-phenylene benzobisthiazole) (PBZT) has been thought to be a manifestation of the sheetlike

hydrogen bonding.³ PIPD, a rigid-rod polymeric fiber with the highest compressive strength for a polymeric material to date,⁴ is thought to form a bidirectional network of hydrogen bonds.⁵ With *ab initio* computational techniques, the intermolecular hydrogen-bonding energy per PIPD repeat unit was calculated to be -22.6 kcal/mol.⁶ The structure and properties of methyl pendant poly(*p*-phenylene benzobisimidazole) (MePBI), which forms a sheetlike arrangement of hydrogen bonds, have been reported elsewhere.⁷ The compressive strengths and torsional moduli of MePBI and PIPD are greater than those of other rigid-rod polymeric fibers that do not have the capacity to form intermolecular hydrogen bonds. Attempts have been made to introduce hydrogen bonding in PBZT through the incorporation of hydroxy groups on the phenyl ring.⁸ The compressive strength of this system (i.e., dihydroxy poly(*p*-phenylene benzobisthiazole), DiOHPBZT; see Fig. 1 for the chemical structures) is lower than that of the unmodified PBZT. The lack of improvement in compressive strength has been attributed

Contribution from the March 2000 Meeting of the American Physical Society—Division of Polymer Physics, Minneapolis, Minnesota

The views and conclusions contained herein are those of the authors and should not be interpreted as necessarily representing the official policies or endorsements, either expressed or implied, of the Air Force Office of Scientific Research or the U.S. Government.

Correspondence to: S. Kumar (E-mail: satish.kumar@textiles.gatech.edu) or K. I. Jacob (E-mail: Karl.Jacob@textiles.gatech.edu)

Journal of Polymer Science: Part B: Polymer Physics, Vol. 38, 3053–3061 (2000)
© 2000 John Wiley & Sons, Inc.

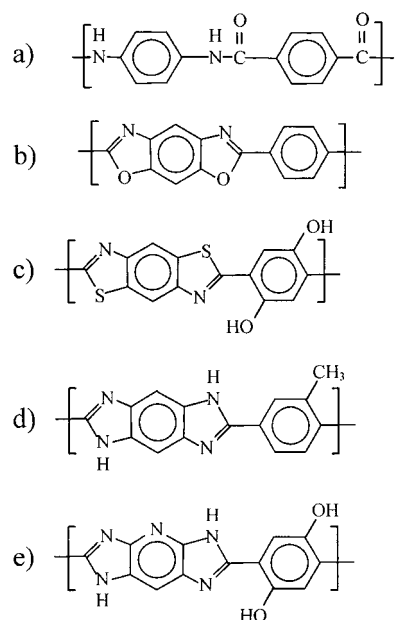


Figure 1. Chemical structures of the high-performance fibers (a) PPTA, (b) PBO, (c) DiOHPBZT, (d) MePBI, and (e) PIPD.

to the formation of intramolecular, rather than intermolecular, hydrogen bonds.⁸ Efforts to cleave the intramolecular hydrogen bonds via chemical means were reportedly unsuccessful. Based on *ab initio* calculations, the intramolecular hydrogen-bonding strength in dihydroxy poly(*p*-phenylene benzobisoxazole) (DiOHPBO) was estimated to be quite significant (−11.7 kcal/mol).⁹ In this article, the influence of intermolecular and intramolecular hydrogen-bond formation on the mechanical and physical properties of high-performance fibers is evaluated and discussed.

SIMULATION PROCEDURE

For all *ab initio* computations, the Dmol module within the InsightII 95.0 (MSI, San Diego, CA) suite of programs was used. The Dmol code is based on density functional theory (DFT), which uses the principle that all ground-state properties can be expressed as a function of electron density. The functional that describes the exchange-correlation energy is of primary importance in calculating the hydrogen-bond energy. The simplest functional uses the local density approximation based on the exchange-correlation energy of a uniform electron cloud. However, this approach

does not accurately predict the bond energies for weakly hydrogen-bonded systems, as the electron cloud is typically not uniform in these systems. Consequently, functionals that take into account the nonuniformity of an electron cloud are necessary. In this work, the Perdew–Wang generalized gradient approximation for the correlation functional and the Becke gradient corrected exchange functionals were used. A double-numeric basis set with polarization functions was also used in all optimizations. Dmol requires the use of a numeric integration grid. A medium integration grid was used for all calculation in this work. The inner core electrons were frozen to reduce the computational time. This simplification was tested and found to influence the absolute value of the final binding energy achieved by optimization but leave the calculated energy difference unchanged.

To calculate the torsional barriers associated with phenyl ring rotation in the polymer repeat units, full geometry optimization was performed with the torsional angles fixed at several positions. Intramolecular hydrogen-bond strengths were estimated according to the procedure of Trohalaki et al.⁹ In summary, unconstrained geometry optimization was performed on small molecular analogues of the polymer repeat unit (Table I), allowing both the hydroxy/phenyl-ring torsion and phenyl-ring/heterocycle torsion to reach their respective minimum energy positions. With the geometry optimized, the hydroxy/phenyl-ring torsional angle was rotated 180° and constrained; the phenyl-ring/heterocycle torsion was also constrained in its optimized position. Geometry optimization was then performed again on the constrained molecule. Because there was no energy change with the rotation of the hydroxy group by 180° in phenol, the difference in energy between the two conformations was taken to be the strength of the intramolecular hydrogen bond.

As the Dmol code within InsightII 95.0 does not have the ability to apply three-dimensional periodic boundary conditions to a system, the interaction energy between chains was estimated as follows: Model compounds, presented in Table II, were placed in proximity to one another in accordance with their spatial arrangement in the crystalline lattice and the conformation dictated by surrounding molecules. Crystalline structures have been reported for PPTA,³ MePBI,⁷ and PIPD.⁵ The head and tail atoms were fixed in space to prevent molecular conformations impossible to realize in the bulk polymer. In addition, torsional angles were fixed to prevent any devia-

Table I. Calculated Intramolecular Hydrogen-Bonding Energies for the Various Model Structures

Representative Polymer	Model Structure	Hydrogen-Bond Energy (kcal/mol)
Hydroxy-PBO		-11.8 (-11.7) ⁹
Hydroxy-PBZT		-12.8
Hydroxy-PBI		-14.6
PIPD		-14.7

tion from the conformation in the crystal. The atoms least involved in the intermolecular interaction, that is, those facing away from the adjacent molecule, were chosen to constrain the torsional angle. As proposed by Hageman et al.,⁶ to isolate the energy associated with the formation of intermolecular hydrogen bonds, we replaced the N—H groups in PIPD, MePBI, and PPTA with oxygen, such that the propensity to form hydrogen bonds was eliminated. The following

Table II. Model Structures Used for Calculating Intermolecular Hydrogen-Bonding Energies

Representative Polymer	Model Structure
PPTA	
MePBI	
PIPD	

steps were involved in calculating the intermolecular hydrogen-bond strength:

1. Calculate the energy ($E_{\text{tot-NH}}$) of two NH-containing, hydrogen-bonded molecules, as they are present in the crystal.
2. Calculate the gas-phase energy of the NH-containing molecule (i.e., the energy when the molecules are well-separated from one another). Sum the energies of the two molecules ($E_{\text{gas-phase-NH}}$).
3. Calculate the energy ($E_{\text{tot-O}}$) of the two O-containing molecules constrained in the original crystal structure position, as for the calculation of $E_{\text{tot-NH}}$ in step 1.
4. Calculate the gas-phase energy of the O-containing molecule. Sum the energies of the two molecules ($E_{\text{gas-phase-O}}$).
5. From these calculations, the energy of the hydrogen bond is determined as follows:

$$E_{\text{H-bond}} = (E_{\text{tot-O}} - E_{\text{gasphase-O}}) - (E_{\text{tot-NH}} - E_{\text{gasphase-NH}})$$

RESULTS AND DISCUSSION

The phenyl rotational barrier in PBZT was investigated¹⁰ with *ab initio* techniques at the re-

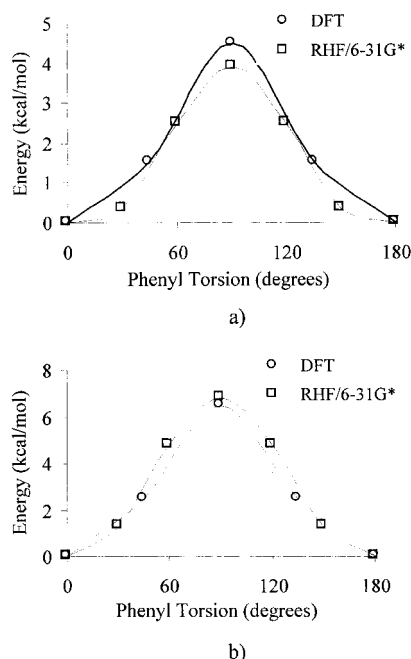


Figure 2. Torsional energy barriers in (a) PBZT and (b) PBO obtained from DFT calculations. Data for the RHF/6-31G* calculations taken from the literature^{9,10} are also presented for comparison.

stricted Hartree–Fock (RHF), self-consistent field level. Specifically, a 6-31G* double- ζ basis set, with polarization functions on non-hydrogen atoms, was employed. At the maximum and minimum of the energy barrier, single-point calculations with second-order Møller–Plesset perturbation theory (i.e., MP2) were undertaken to correct for electron correlation. For comparison, we performed analogous calculations on the same structure with Dmol. The results are presented in Figure 2(a). At the MP2/6-31G*//RHF/6-31G* level, the rotational barrier was calculated to be 3.90 kcal/mol.¹⁰ Without correction for electron correlation (i.e., at the RHF/6-31G* level), the barrier increased to 4.04 kcal/mol.¹⁰ In this work, the rotational barrier was calculated to be 4.51 kcal/mol. This result is representative in that the numbers obtained from the DFT calculations tended to compare more favorably to the RHF/6-31G* level. Inasmuch as errors of ± 1 kcal/mol are fairly common in comparing calculated heats of fusion with experimental values,¹¹ such a disparity may not be so important in many cases. Similarly, the rotational barrier of PBO was calculated for this work and compared with previously reported data [Fig. 2(b)].⁹

Table I reports the values for the intramolecular hydrogen-bonding strengths for various sys-

tems, as measured in this work. Also included are the value previously reported⁹ for the hydroxy-PBO model compound, obtained with a 6-31+G(2d, 2p) extended basis set on the nitrogen, hydrogen, and oxygen involved in the hydrogen bond, and the MP2 correction. Fair agreement exists between the two values. The strength of the intramolecular hydrogen bond in DiOHPBZT may explain the ineffectiveness of the attempts to break these bonds.⁸ In comparing PIPD to DiOHPBZT, PIPD forms a stronger intramolecular hydrogen bond by roughly 2 kcal/mol. Because intermolecular hydrogen bonding is also occurring in PIPD, it would seem that the formation of one type of hydrogen bond (i.e., intramolecular or intermolecular) would not preclude the formation of the other.

While crystal structures of PIPD and MePBI have been presented,^{5,7} the crystal structure determination of DiOHPBZT is hampered by the fact that relatively few diffraction peaks are available in wide-angle X-ray diffractograms (WAXDs) of these fibers (Fig. 3). The equatorial DiOHPBZT reflections may be indexed to a primitive unit cell of dimensions $a = 6.43$ Å, $b = 3.48$ Å, and $\gamma = 105.6^\circ$. This primitive unit cell can then be expressed as a larger, nonprimitive unit cell containing two repeat units at positions (0, 0) and ($\frac{1}{2}$, $\frac{1}{2}$). The dimensions of the nonprimitive DiOHPBZT unit cell would then be $a = 12.86$ Å and $b = 3.48$ Å, where γ is now 90° , as compared with $a = 12.60$ Å, $b = 3.48$ Å, and $\gamma = 90^\circ$ for PIPD. An obvious difference in the two crystal structures is that the a lattice dimension of the DiOHPBZT crystal is greater. This may be construed, perhaps naively, to result from weaker intermolecular interactions or less efficient packing.

On the basis of the crystal structures of PPTA,³ MePBI,⁷ and PIPD,⁵ the intermolecular hydrogen-bond strengths calculated with *ab initio* techniques are given in Table III. The repeat units of PIPD and PPTA have four groups involved in hydrogen bonding, whereas MePBI has two. Therefore, the hydrogen-bonding energy in Table III is given per mole of hydrogen bonds formed and per mole of repeat units. The energy associated with the hydrogen bond in PIPD was calculated to be -5.20 kcal/mole. As each PIPD repeat unit is involved in four hydrogen bonds, this results in a hydrogen-bonding energy per repeat unit of -20.8 kcal/mol. Clearly, any error involved in calculating the energy of one hydrogen bond is multiplied by a factor of four with this process. Nonetheless, fairly good agreement with

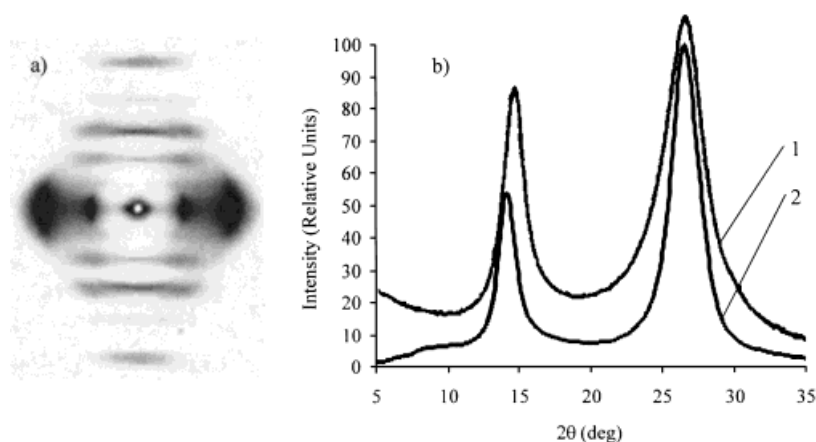


Figure 3. (a) WAXD of DiOHPBZT and (b) equatorial scans of tension heat-treated (1) PIPD fiber (adapted from ref. 5) and (2) DiOHPBZT fiber.

the work of Hageman et al.⁶ was obtained, where the hydrogen-bonding energy per repeat unit is reported to be -22.6 kcal/mol.

As mentioned previously, PIPD can form both intermolecular and intramolecular hydrogen bonds. An attempt was made to determine if a change in the intermolecular hydrogen-bonding strength could be calculated when the intramolecular hydrogen bond was severed. This was modeled by the hydroxy groups being rotated on the PIPD repeat unit by 180° and then being constrained in that position. In this way, the intramolecular hydrogen bond was effectively severed, but the intermolecular hydrogen bond was retained. After the cleaving of the intramolecular hydrogen bond, the intermolecular hydrogen-bond energy was calculated and found to be weaker by approximately 1 kcal/mol of hydrogen bonds. As this difference is close to the error expected for such calculations, it can be concluded that no significant difference in intermolecular hydrogen-bonding strength is expected with the cleaving of the intramolecular hydrogen bond.

Table III. Calculated Intermolecular Hydrogen-Bonding Energies of Small Molecular Analogues of Several High-Performance Polymer Systems

	E (kcal/mol Hydrogen Bond)	E (kcal/mol Repeat Units)
PPTA	-6.24	-25.0
MePBI	-8.85	-17.7
PIPD	-5.20	-20.8 (22.6) ⁶

The results imply that intramolecular hydrogen bonding is not necessarily at fault in the lack of intermolecular hydrogen bonding in DiOHPBZT. Rather, the chemical structure of the heterocycle in DiOHPBZT and the consequent packing of the chains within the crystal are most likely responsible for the lack of intermolecular hydrogen bonding. Figure 4 qualitatively illustrates the relative positioning of neighboring chains and consequent hydrogen-bond formation in DiOHPBZT and PIPD. As illustrated in this figure, PIPD can form a continuous network of hydrogen bonds via the hydroxy group and local secondary amine, even though the hydroxy group is intramolecularly associated with the tertiary amine. For DiOHPBZT, tertiary amines must be directed toward one another [Fig. 4(c)] to form an intermolecular hydrogen bond via the hydroxy group, but the intramolecular hydrogen bond must also be accommodated. If amine groups were directed as shown in Figure 4(b), a means of forming intermolecular hydrogen bonding would be less obvious. The formation of intermolecular hydrogen bonds via hydroxy groups on adjacent chains is conceivable; however, a more detailed crystalline model would be necessary to determine if such bonds were forming. Significant hydroxy pendant interaction is not thought to be occurring in PIPD.

Table III shows that PIPD has a greater hydrogen-bonding association energy per repeat unit than MePBI. A greater number (i.e., four) of comparatively weak hydrogen bonds exist in PIPD, whereas fewer (i.e., two) but stronger

hydrogen bonds are present in MePBI. A plot of hydrogen bond strength versus compressive strength is given in Figure 5. The hydrogen-bond strength of PBO is taken to be zero, as there is no hydrogen bonding in this system. Compressive strength data has been taken from the literature. The compressive strength of PBO and MePBI was measured by the recoil compressive test,¹² whereas the PIPD compressive strength was measured using the composite²³ and Raman²⁴ tests. A trend of increasing compressive strength with increasing intermolecular association is shown in Figure 5. While this is consistent with the theories proposed for compressive failure in highly oriented fibers,^{13,14} two conditions, as discussed below, must be satisfied for this trend to be meaningful.

The shear modulus between polymer chains, g , plays a significant role in the various theories on compressive strength and is given by:

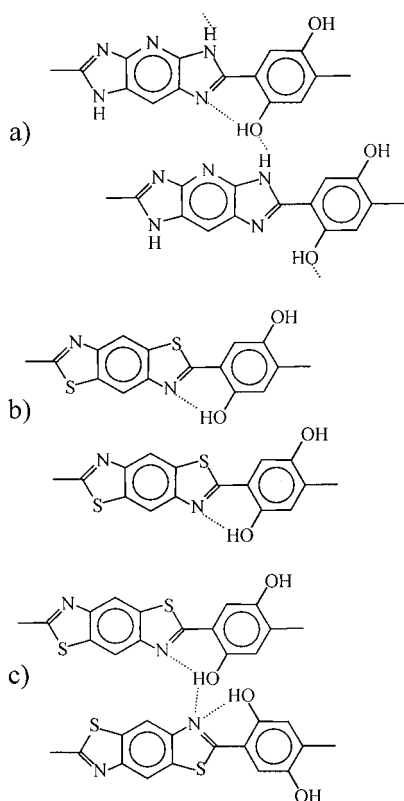


Figure 4. Suggested arrangement of the hydrogen bonds in (a) PIPD, (b) DiOHPBZT and (c) DiOHPBZT. As discussed in the text, the last arrangement represents a hypothetical but most likely impractical molecular arrangement allowing for intermolecular hydrogen bonding in DiOHPBZT.

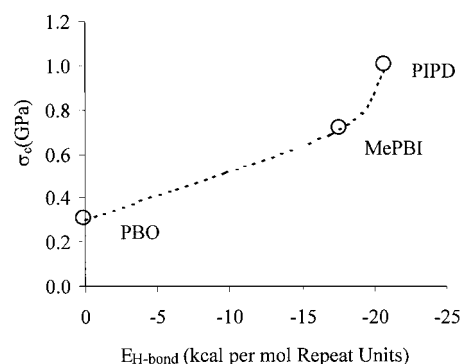


Figure 5. Relationship between the strength of the intermolecular interactions and the measured compressive strength. The compressive strength data were taken from the literature.^{1,7,23,24} PBO does not have the ability to hydrogen bond, so $E_{\text{H-bond}}$ was set to zero for illustrative purposes.

$$g = C_{44} = C_{2323} = \frac{1}{V_o} \left. \frac{\partial^2 U}{\partial \epsilon_{23} \partial \epsilon_{23}} \right|_{T, \epsilon_{23}}$$

where ϵ_{23} is a shear strain acting on a radially oriented plane in the direction of the fiber axis and U is the strain energy density. Single-point calculations of hydrogen-bonding energy may not provide enough information to correlate to shear modulus. Several calculations must be performed when shearing one molecule with respect to its neighbor. The correlation can be sustained if the hydrogen bond is the predominant contributor (and proportional) to $\partial^2 U / \partial \epsilon_{23} \partial \epsilon_{23}$.[†]

In polymer systems with planar hydrogen bonding, planes offering lower resistance to shear would be present. These planes would be expected to dictate compressive strength. However, if transverse isotropy existed on a scale larger than several unit cells or if a crystallite had rotational anisotropy, all shear planes would be sampled where planar hydrogen bonds contributed to the compressive strength of the fiber.

A hydrogen-bonded, sheetlike structure has been predicted for MePBI.⁷ PPTA also forms a sheetlike arrangement of hydrogen bonds. The higher compressive strength of MePBI relative to the strength of PPTA suggests that hydrogen-bond formation may not be the only factor involved in influencing compressive strength, particularly because the intermolecular hydrogen-bonding strength in PPTA is higher than in

[†] That is, if trends in the series expansion $\partial^2 U / \partial \epsilon_{23} \partial \epsilon_{23}$ remain unchanged upon truncation after the first term.

MePBI and in PIPD (Table III). Other factors, such as chain flexibility (i.e., conformational flexibility) and consequent morphological differences, may also influence the compressive strength of these materials, as discussed elsewhere.⁷

A linear correlation has been observed between the compressive strength and torsional modulus for a number of highly oriented fibers.^{13,15} The fiber torsional modulus can give a macroscopic measure for the shear modulus between chains, but it is greatly influenced by voids or any transverse texture present in the fiber. If a fiber is transversely isotropic, the measured torsional modulus and average interchain shear modulus should be comparable. However, this most likely is not the case in PPTA^{16,17} and PBO,¹⁸ as such isotropy was not observed in these fibers. As mentioned previously, PPTA forms a sheetlike, hydrogen-bonded structure, with the direction of the crystalline *b* axis (and hydrogen-bonded sheets) oriented radially.³ In PBO, the *a* axis is oriented radially.¹⁸ High-modulus PPTA fiber (i.e., KevlarTM 149) conceivably would have better molecular orientation and crystal perfection than the lower modulus PPTA fibers (i.e., KevlarTM 29 and 49). Moreover, an enhanced transverse texture would be expected with improved crystal perfection. In the lower modulus PPTA fibers, the crystal structures would be expected to contain a greater number of imperfections and degree of misorientation, but they are still known to retain transverse texture.¹⁹ Compressive strength and torsional modulus data for various high performance fibers is listed in Table IV.

The temperature-dependent torsional moduli of MePBI, PBO, and PPTA (i.e., KevlarTM 49 and KevlarTM 149) are presented in Figure 6. The higher torsional modulus of MePBI can be attributed to the formation of intermolecular hydrogen bonds within the structure. Similar reasoning would suggest that KevlarTM 49 and KevlarTM 149 should also exhibit higher torsional moduli due to hydrogen bonding. In fact, the highly oriented KevlarTM 149 fiber shows the lowest torsional modulus for the PPTA fibers, whereas the less ordered KevlarTM 29 shows the highest. This may be explained in terms of the lateral texture exhibited in these materials. The presence of lateral texture in a weakly associating system, such as PBO, would be expected to be inconsequential, in that van der Waals interactions are at work regardless of crystallite orientation. Thus, preferential transverse orientation would not significantly influence the torsional modulus in such systems.

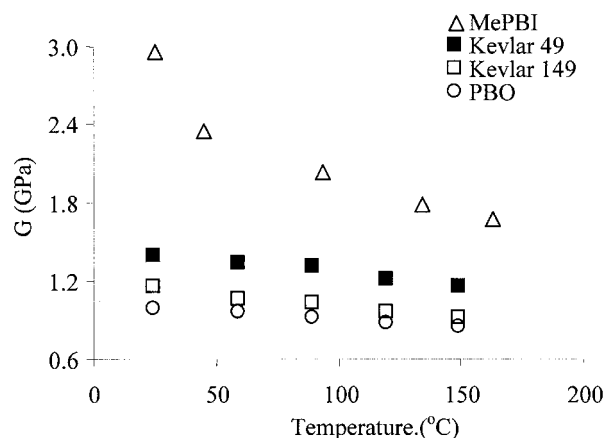


Figure 6. Temperature-dependent torsional modulus of MePBI, PBO, and PPTA (i.e., KevlarTM 49 and KevlarTM 149). The values for PBA and PPTA were taken from ref. 22. The MePBI torsional modulus was measured according to the procedure described in ref. 22.

Similar conclusions can be made in terms of the observed decrease in torsional modulus as a function of temperature, as presented in Figure 6. Variable-temperature Fourier transform infrared has been applied to aliphatic, amorphous polyamides²⁰ and the aromatic polyamide PPTA²¹ in monitoring hydrogen bonding as a function of temperature. For aliphatic polyamides, a systematic shift to a higher frequency and a decrease in the intensity of the N—H absorption band with temperature was attributed to a decrease in the average strength of the hydrogen bond. In PPTA, the peak position remained constant up to temperatures as high as 300 °C, with the only spectral change being a decrease in the intensity with increasing temperature. Inasmuch as the frequency of the N—H stretching mode is dictated primarily by distance and geometry,²⁰ conformational rigidity would appear to manifest itself in the increased thermal stability of the hydrogen bond. Hydrogen-bonding strength in MePBI⁷ has also been observed to decrease with temperature. This may in part explain the observation that MePBI loses over 50% of its torsional stiffness on heating to 150 °C. In PBO, where van der Waals interactions are predominant, a dramatic drop in the strength of the intermolecular interaction as a function of temperature is not expected, which would result in the observed retention of torsional stiffness. Behavior resembling that of MePBI was not observed in the PPTA fibers, even though hydrogen bonding is present in PPTA. This also is explained in terms of the radial texture in PPTA,

which causes a torsional strain to sample planes primarily bonded via van der Waals interactions. Thus, behavior more analogous to PBO may be expected.

Although a stronger intermolecular association can increase tensile modulus and strength,¹⁴ compressive strength,^{13,14} and torsional modulus, Figure 7 presents another influence of such interactions. Specifically, increasing the intermolecular interactions appears to increase density. Both the theoretical density, calculated from the crystal structure, and the experimental density showed similar increases. Only rigid-rod polymers containing carbon, oxygen, and nitrogen were plotted. Systems with heavier elements tend to increase density, regardless of increasing intermolecular interactions (e.g., the sulfur in PBZT, $\rho_{\text{theoretical}} = 1.71 \text{ g/cm}^3$, $\sigma_c^{\text{recoil}} = 0.3 \text{ GPa}$). Contrary to the trend presented in Figure 7, compressive strength decreased with increasing density in carbon fibers.² However, the primary factors influencing density in the carbon fibers were void content and graphitic order. The similarity in the slopes of the two least-squares fitted lines of Figure 7 suggests that the void content in these systems does not play a significant role. Rather, a phenomenological argument of increased association leading to increased density would apply. Thus, one may wish to design systems that would improve intermolecular interactions without an increase in density. Systems taking advantage of longer range interactions (e.g., ionic interactions), while disrupting efficient packing (e.g., through bulky side groups), may be desirable.

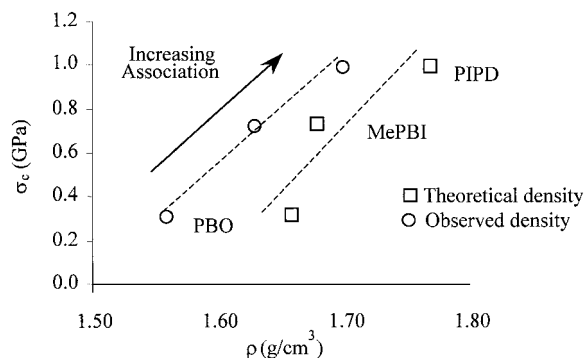


Figure 7. Relationship between the compressive strength (σ_c) and density (ρ) of various rigid-rod polymers. All the data were taken from refs. 1, 7, 23, 24, and 26 and Toyobo technical data on Zylon™.

Table IV. Compressive Strength and Torsional Modulus Values of Some High-Performance Fibers

Fiber	Compressive Strength (GPa)	Torsional Modulus (GPa)
PBZT	0.3 ¹	1.2 ^{15,22}
PBO	0.2–0.3 ¹	1.0 ²²
PPTA		
Kevlar™ 29	N/A	1.9 ²²
Kevlar™ 49	0.35–0.45 ¹	1.4, 1.5 ^{15,22}
Kevlar™ 149	0.32–0.46 ¹	1.1 ²²
OH-PBZT	0.03–0.42 ⁸	N/A
MePBI	0.71 ⁷	3.0 ⁷
PIPD	1.0 ^{23,24}	~ 3 ²⁵

This effort was partially sponsored by the Air Force Office of Scientific Research, Air Force Materials Command, United States Airforce, under Grant F49620-00-1-0147. The U.S. Government is authorized to reproduce and distribute reprints for Government purposes, notwithstanding any copyright notation thereon.

REFERENCES AND NOTES

- Kozey, V. V.; Jiang, H.; Mehta, V. R.; Kumar, S. *J Mater Res* 1995, 10, 1044.
- Kumar, S.; Helminiak, T. *Mater Res Soc Symp Proc* 1989, 134, 363.
- Northolt, M. G. *Eur Polym J* 1974, 10, 799.
- Lammers, M.; Klop, E. A.; Northolt, M. G.; Sikkema, D. J. *Polymer* 1998, 39, 5999.
- Klop, E. A.; Lammers, M. *Polymer* 1998, 39, 5987.
- Hageman, J. C. L.; van der Horst, J. W.; de Groot, R. A. *Polymer* 1999, 40, 1313.
- Jenkins, S.; Jacob, K. I.; Polk, M. B.; Kumar, S.; Dang, T.; Arnold, F. E. *Macromolecules*, in press.
- Tan, L.-S.; Arnold, F. E.; Dang, T. D.; Chuah, H. H.; Wei, K. H. *Polymer* 1994, 35, 14.
- Trohalaki, S.; Yeates, A. T.; Dudis, D. S. In *Modeling the Hydrogen Bond*; Smith, D. A., Ed.; ACS Symposium Series 569; American Chemical Society: Washington, DC, 1994; p 269.
- Trohalaki, S.; Dudis, D. S. *Polymer* 1995, 36, 911.
- Hehre, W. J.; Radom, L.; Schleyer, P. V. R.; Pople, J. A. *Ab Initio Molecular Orbital Theory*; Wiley Interscience: New York, 1986.
- Allen, S. R. *J Mater Sci* 1987, 22, 853.
- DeTeresa, S. J.; Porter, R. S.; Farris, R. J. *J Mater Sci* 1985, 20, 1645.
- Northolt, M. G.; Van der Hout, R. *Polymer* 1985, 26, 310.
- DeTeresa, S. J.; Porter, R. S.; Farris, R. J. *J Mater Sci* 1987, 23, 1886.

16. Dobb, M. G.; Johnson, D. J.; Saville, B. P. *J Polym Sci Polym Phys Ed* 1977, 15, 2201.
17. DeTeresa, S. J. U.S. Air Force Wright Aeronautical Laboratory, Technical Report 85-4012, 1985.
18. Kitagawa, T.; Murase, H.; Yabuki, K. *J Polym Sci Part B: Polym Phys* 1998, 36, 39.
19. Warner, S. B. *Macromolecules* 1983, 16, 1564.
20. Skrovanek, D. J.; Howe, S. E.; Painter, P. C.; Coleman, M. M. *Macromolecules* 1985, 18, 1676.
21. Siesler, H. W.; Holland-Moritz, K. *Infrared and Raman Spectroscopy of Polymers*; Marcel Dekker: New York, 1980; Vol. 4.
22. Mehta, V. R.; Kumar, S. *J Mater Sci* 1994, 29, 3658.
23. Sikkema, D. J. *The Fiber Society Book of Abstracts*; Mulhouse: France, 1997.
24. Sirichaisit, J.; Young, R. J. *Polymer* 1999, 40, 3421.
25. Lammers, M. Ph.D. Thesis, Swiss Federal Institute of Technology, Zurich, 1998.
26. Fratini, A. V.; Lenhert, P. G.; Resch, T. J.; Adams, W. W. *Mater Res Soc Symp Proc* 1989, 134, 431.